Journal of Molecular Catalysis A: Chemical 317 (2010) 81–88

Contents lists available at ScienceDirect

Journal of Molecular Catalysis A: Chemical

journal homepage: www.elsevier.com/locate/molcata

Synthesis of efficient and reusable catalyst of size-controlled Au nanoparticles within a porous, chelating and intelligent hydrogel for aerobic alcohol oxidation

Yao Wang, Rui Yan, Jianzheng Zhang, Wangqing Zhang*

Key Laboratory of Functional Polymer Materials of Ministry of Education, Institute of Polymer Chemistry, Nankai University, No. 94, Weijin Road, Tianjin 300071, China

ARTICLE INFO

Article history:
Received 20 July 2009
Received in revised form 18 October 2009
Accepted 22 October 2009
Available online 31 October 2009

Keywords:
Alcohol oxidation
Au nanoparticles
Catalysis
Hydrogel
Poly(*N*-isopropylacrylamide)

ABSTRACT

Synthesis of size-controlled Au nanoparticles for aerobic alcohol oxidation within a porous, chelating and intelligent hydrogel of poly(*N*-isopropylacrylamide)-*co*-poly[2-methacrylic acid 3-(bis-carboxymethylamino)-2-hydroxypropyl ester] (PNIPAM-*co*-PMACHE) is studied. The PNIPAM-*co*-PMACHE hydrogel is demonstrated to be a suitable scaffold, within which Au nanoparticles with size ranging from 2.6 to 6.3 nm are synthesized by reducing the Au precursor of $HAuCl_4$ with different reducing agents. The synthesized composite of the hydrogel and the encapsulated Au nanoparticles is thermoresponsive, which can reversibly deswell/swell at the volume-phase-transition temperature (VPTT) at 27 °C. The encapsulated Au nanoparticles keep stable during the reversible deswelling/swelling of the thermoresponsive hydrogel/Au composite. The catalysis of the thermoresponsive composite is tested employing aerobic alcohol oxidation as model reaction and it is found that the catalytic activity of the thermoresponsive composite is strongly dependent on the size of the encapsulated Au nanoparticles. Besides, it is found that the thermoresponsive composite is catalytically efficient for aerobic alcohol oxidation partly since the reactant of alcohol is highly concentrated within the hydrogel matrix through the reversible deswelling and partly since the reactant of alcohol can be activated through the strong hydrogen bonding between the alcohol molecules and the poly(*N*-isopropylacrylamide) segment. And furthermore, the reversible deswelling/swelling of the thermoresponsive composite provides great convenience for catalyst recycling.

1. Introduction

Alcohol oxidation to aldehyde or ketone is one of the pivotal functional group transformations in organic chemistry [1]. Generally, oxidation is performed using stoichiometric amount of transition metal oxidants or sulfoxides and this stoichiometric oxidation produces a large amount of undesirable products [1], which becomes intolerable in today's environmentally conscious world. Thus, development of environmentally friendly catalytic oxidation of alcohol with molecular oxygen at atmospheric pressure in green solvent is an important and urgent work [2–4]. Recently, aerobic alcohol oxidation employing heterogeneous noble metal nanocatalyst has stimulated great interest since it avoids using toxic and large amount of oxidizing reagent and no by-product other than water is produced. Of all the noble metal nanocatalysts such as Au [4–8], Pd [9–11], Pt [12,13] and Rh [14,15], Au nanocatalyst is deemed to have promising potential partly since it is not prone to leaching as a result of overoxidation and partly due to its high efficiency. Up to now, various heterogeneous Au nanocatalysts immobilized on inorganic metal oxides such as CeO_2 [7], TiO_2 [16], or MnO_2 [17] or stabilized with functional polymers such as poly(*N*-vinyl-2-pyrrolidone) [2], poly[2-(2-ethoxy)ethoxyethyl vinyl ether] [4] and poly[*N*,*N*-dimethylacrylamide-*co*-2-(methylthio)ethylmethacrylate-*co*-*N*,*N*′-methylenebisacrylamide] [18] have been proposed. It is generally concluded that the catalyst preparation method, the size of Au nanoparticles and the nature of catalyst support are important to determine the efficiency of Au catalyst. For example, Tsukuda and co-workers found that the turnover frequency (TOF) value of Au nanocatalyst decreases with the increase in the size of Au nanoparticles in the range from 3 to 10 nm [19]. Louis and co-workers found that the catalyst of Au nanoparticles immobilized on reductive metal oxides such as CeO_2 or TiO_2 is more efficient than those on Al_2O_3 [20].

Hydrogel is three-dimensional network of cross-linked polymer, which can swell in aqueous medium. The three-dimensional network of hydrogel is deemed to be a suitable scaffold for *in situ* synthesis of noble metal nanoparticles since the swollen hydrogel provides free space for nucleation and growth of noble metal nanoparticles [21–24]. Up to now, the poly(*N*-isopropylacrylamide) (PNIPAM) based hydrogel, which can reversibly deswell/swell at the volume-phase-transition temperature (VPTT) [25–28], has

* Corresponding author. Tel.: +86 22 23509794; fax: +86 22 23503510.
E-mail address: wqzhang@nankai.edu.cn (W. Zhang).

1381-1169/$ – see front matter © 2009 Elsevier B.V. All rights reserved.
doi:10.1016/j.molcata.2009.10.026

been used to synthesize Au [21], Ag [22], and Pd [23] nanoparticles. When the catalyst of noble metal nanoparticles is immobilized within the PNIPAM-based hydrogel matrix, it is expected to have a special advantage of easy separation and reuse through the reversible deswelling/swelling of the thermoresponsive hydrogel. Up to now, generation of catalytically active metal nanoparticles within swollen polymer network including thermoresponsive microgel is reported [29–31]. However, size-controlled synthesis of metal nanoparticles within a bulk thermoresponsive hydrogel and their application in catalysis is rarely reported [23,32].

In a recent manuscript [33], we have demonstrated that the Pd-catalyzed C–C cross-coupling reaction within a porous, chelating and intelligent hydrogel of poly(*N*-isopropylacrylamide)-*co*-poly[2-(bis-carboxymethylamino)-2-hydroxypropyl methacrylate] (PNIPAM-*co*-PMACHE) is very efficient. The reason is partly ascribed to the Pd catalyst and reactants being highly concentrated within the hydrogel matrix through its reversible deswelling/swelling. We believe that the method to concentrate reactants and catalyst within thermoresponsive hydrogel matrix will broad a new way to accelerate reaction. In the present study, synthesis of Au nanocatalyst encapsulated within the PNIPAM-*co*-PMACHE hydrogel matrix for aerobic alcohol oxidation is studied and three main conclusions are made. First, synthesis of size-controlled Au nanoparticles within the PNIPAM-*co*-PMACHE hydrogel is easily achieved just by adjusting reducing agents, and the encapsulated Au nanoparticles keep stable during the reversible deswelling/swelling of the thermoresponsive hydrogel/Au composite. Second, the catalyst of encapsulated Au nanoparticles is highly efficient for aerobic alcohol oxidation. The reason is partly ascribed to the highly concentrated reactants and Au nanocatalyst within the hydrogel and partly ascribed to the activated alcohol through strong hydrogen bonding between alcohol and the PNIPAM segment [34–36]. Third, the hydrogel/Au composite can be easily recovered and reused because it can reversibly deswell/swell. Herein, it should be pointed out that the catalyst of Au nanoparticles instead of Pd nanoparticles is employed since it is found that the encapsulated Au nanocatalyst is more efficient for aerobic alcohol oxidation than the encapsulated Pd nanocatalyst [33] (Figs. S1–2, seeing in Supporting Information).

2. Experimental

2.1. Materials

The PNIPAM-*co*-PMACHE hydrogel, which contains a chelating ligand of iminodiacetic acid (IDA) in the PMACHE segment and a thermoresponsive segment of poly(*N*-isopropylacrylamide) (PNIPAM), was synthesized by copolymerization of *N*-isopropylacrylamide (NIPAM) and 2-(*bis*-carboxymethylamino)-2-hydroxypropyl methacrylate (MACHE) employing *N*,*N*′-methylenebisacrylamide (BIS) as cross-linker, $K_2S_2O_8$ as initiator, and *N*,*N*,*N*′,*N*′-tetramethylethylenediamine (TEMED) as accelerator in the water/THF mixture at ~28 °C for 4 h. The detailed synthesis of the PNIPAM-*co*-PMACHE hydrogel can be found as discussed elsewhere [33]. $HAuCl_4{\cdot}3H_2O$ (>99.9%), sodium citrate (>99%), $NaBH_4$ (>98.9%), and 1-phenylethanol (>99%) were used as received. Double-distilled water was used in the present experiment.

2.2. Synthesis of size-controlled Au nanoparticles within the PNIPAM-co-PMACHE hydrogel

Au nanoparticles encapsulated within the PNIPAM-*co*-PMACHE hydrogel were synthesized firstly by coordination between the Au precursor of $HAuCl_4$ with the chelating PMACHE segment and followed by reduction with a suitable reducing agent. In the present study, four kinds of Au nanoparticles with different sizes were synthesized by reducing $HAuCl_4$ with $NaBH_4$, sodium citrate and H_2, respectively. For synthesis of 2.6 nm Au nanoparticles, to a glass beaker 15 g of PNIPAM-*co*-PMACHE hydrogel and 6.0 mL of 1.0 mmol/L $HAuCl_4$ aqueous solution were added, where the molar ratio of the chelating ligand of IDA to Au was set at 8/1. The mixture was kept at room temperature for ~15 min with stirring. Subsequently, 4.0 mL of 7.5 mmol/L $NaBH_4$ aqueous solution was added. Lastly, the mixture was kept at room temperature for about 3 h with stirring. The synthesis of 4.0 nm Au nanoparticles is as similar as those of the 2.6 nm Au nanoparticles except that 4.0 mL of 3.0 mmol/L $NaBH_4$ aqueous solution was used as reducing agent. For synthesis of 5.7 nm Au nanoparticles, to a glass beaker equipped with a reflux condenser 15 g of PNIPAM-*co*-PMACHE hydrogel and 6.0 mL of 1.0 mmol/L $HAuCl_4$ aqueous solution were added. The mixture was firstly kept at room temperature for ~15 min with stirring and then heated to 100 °C. Subsequently, 4.0 mL of 7.5 mmol/L sodium citrate aqueous solution was added and the mixture was firstly kept at 100 °C for 1 h with stirring and then kept at room temperature for the next use. For synthesis of 6.3 nm Au nanoparticles, to a glass beaker 15 g of PNIPAM-*co*-PMACHE hydrogel and 6.0 mL of 1.0 mmol/L $HAuCl_4$ aqueous solution were added. The mixture was firstly heated to 50 °C, and then H_2 was bubbled for 1 h at rate of 10 cm^3/min, and finally kept at room temperature for the next use.

2.3. Aerobic alcohol oxidation catalyzed by the encapsulated Au nanoparticles within the PNIPAM-co-PMACHE hydrogel

Into a glass vessel equipped with a reflux condenser, the swollen hydrogel/Au composite (15 g, containing 6.0×10^{-4} mmol of Au nanocatalyst), 1-phenylethanol (3.0 mmol) and KOH (9.0 mmol) were added. The mixture was stirred at 80 °C for ~5 min and then oxidation was carried out by bubbling O_2 (ca. 0.05 L/min) at atmospheric pressure. At a given time, 1 g of the reaction mixture was firstly taken out from the glass vessel, and then be immersed in about 20 mL of acetonitrile (CH_3CN) at room temperature, and subsequently analyzed with high performance liquid chromatography (HPLC).

To test the reusability of the hydrogel/Au composite, after the oxidation was completed, the reaction mixture was firstly cooled to room temperature instantly. Subsequently, diethyl ether (3× 20 mL) was added and the product was extracted. The organic phase was decanted, and the collected organic phase was concentrated and analyzed with HPLC and atomic absorption spectrum (AAS). After the deswelled hydrogel/Au composite being kept at room temperature for ~2 h, it reversibly swelled. Then the same amount of 1-phenylethanol (3.0 mmol) was added, and the next run of oxidation was performed under condition as same as the fresh cycle.

2.4. General characterization

Scanning electron microscopy (SEM, Philips XL30) was used to study the surface morphology of the PNIPAM-*co*-PMACHE hydrogel. To observe the real surface morphology of the PNIPAM-*co*-PMACHE hydrogel, the swollen hydrogel was quickly frozen in liquid nitrogen and then freeze-dried in an ALPHA 1-2LD freeze drier for 3 days to remove water completely. The freeze-dried gel was sputtering-coated with a thin gold film and then observed by SEM. Transmission electron microscope (TEM) observation was conducted by using a Philips T20ST electron microscope at an acceleration voltage of 200 kV, whereby a thin piece of the hydrogel/Au composite was deposited onto a piece of copper grid, and then dried at atmospheric pressure. The UV–vis absorption spectra of the hydrogel/Au composite were recorded on a TU-8110 UV-vis spec-

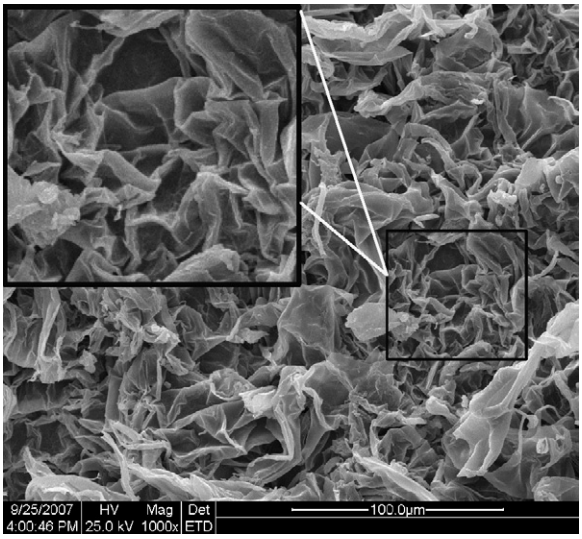

Fig. 1. The SEM image of the PNIPAM-*co*-PMACHE hydrogel.

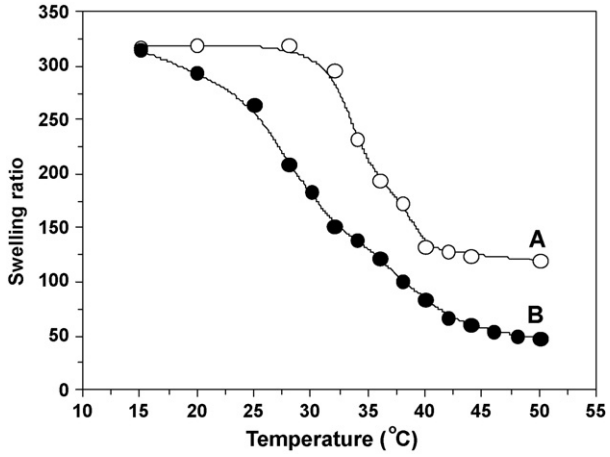

Fig. 2. Temperature dependence of the swelling ratio of the PNIPAM-*co*-PMACHE hydrogel (A) and the composite of the hydrogel and the encapsulated 2.6 nm Au nanoparticles (B) in neutral water.

trophotometer in a standard quartz cell with a path length of 1 cm at a given temperature. The X-ray photoelectron spectroscopy (XPS) analyses were performed with a Kratos Axis Ultra DLD spectrometer employing a monochromated Al Ka X-ray source (1486.6 eV) and a delay line detector (DLD). The Fourier transform infrared spectrometry (FTIR) spectra were recorded on a Bio-Rad FTS-6000 IR spectrometer. HPLC analysis was performed on a LabAlliance PC2001 system equipped with a C18 column and a UV-vis detector using the mixture of CH_3CN and water (6:4 by volume) as eluent. The swelling ratio of the PNIPAM-*co*-PMACHE hydrogel was measured gravimetrically. The hydrogel sample was prepared firstly by immersing a given amount of the fully dried gel in excess amount of water at room temperature for at least 24 h. Then, the swollen hydrogel was put in neutral water at a given temperature for a given time. Subsequently, the hydrogel was weighted after carefully blotting surface water with moistened filter paper. The average value of three measurements was taken for each sample. The swelling ratio was defined as the average value of the hydrogel to that of the fully dried gel. The swelling ratio of the hydrogel/Au composite was measured as similar as that of the hydrogel.

3. Results and discussion

3.1. Synthesis and characterization of the PNIPAM-co-PMACHE hydrogel

The PNIPAM-*co*-PMACHE hydrogel was synthesized as discussed elsewhere [33]. The copolymerization of NIPAM and MACHE affords almost quantitative yield of gel at 28 °C for 4 h. The resultant material is a bulk hydrogel and the hydrogel is apt to be smashed into little fragments by gently stirring (Fig. S3A, seeing in Supporting Information). The chemical composition of the PNIPAM-*co*-PMACHE hydrogel can be found in Ref. [33]. Fig. 1 shows the SEM image of the PNIPAM-*co*-PMACHE hydrogel. Clearly, the hydrogel has a porous structure, which is useful to increase accessibility of the encapsulated Au nanocatalyst. The PMACHE segment affords the chelating ligand of IDA to coordinate with the Au precursor and therefore to immobilize Au nanoparticles within the hydrogel matrix. As to the PNIPAM segment, it possesses three virtues. First, there exists strong hydrogen bonding between the reactant of alcohol and the PNIPAM segment, and therefore to encapsulate alcohol within the PNIPAM-*co*-PMACHE hydrogel matrix. Second, the thermoresponsive hydrogel can deswell/swell reversibly to concentrate alcohol and the encapsulated Au nanocatalyst within the hydrogel matrix and therefore to accelerate the oxidation of alcohol. Third, the reversible deswelling/swelling provides convenient reuse of the hydrogel/Au composite.

As similar as the general PNIPAM-based hydrogels [25–28], the present PNIPAM-*co*-PMACHE hydrogel is thermoresponsive and has a volume-phase-transition temperature (VPTT) at 32 °C as shown in Fig. 2A. That is to say, the hydrogel deswells at temperature above 32 °C and reversibly swells in water when temperature decreases below 32 °C. Besides, the present hydrogel is also pH-responsive due to the zwitterionic pH-responsive segment of PMACHE. The PNIPAM-*co*-PMACHE hydrogel swells at the pH range of 4–10 and deswells out of this pH range [33], which is a little different from the typical thermoresponsive and pH-responsive hydrogel of poly(*N*-isopropylacrylamide-*co*-methacrylic acid) (PNIPAM-*co*-PMAA) [37] or poly(*N*-isopropylacrylamide-*co*-acrylic acid) (PNIPAM-*co*-PAA) [38].

In the previous manuscript [33], it is demonstrated that whether hydrophobic or hydrophilic aryl halides can be encapsulated within the PNIPAM-*co*-PMACHE hydrogel. In the present study, the encapsulation of hydrophobic alcohols such as 1-phenylethanol and benzyl alcohol within the PNIPAM-*co*-PMACHE hydrogel can be optically observed. For example, after benzyl alcohol being added in the hydrogel, the transparent hydrogel becomes opaque at once and the organic phase gradually disappears indicating encapsulation of alcohol within the hydrogel matrix (Fig. S3, seeing in Supporting Information). Up to now, various evidences on hydrogen bonding between alcohol molecules and PNIPAM have been proposed [34–36]. Herein, the hydrogen bonding between the alcohol hydroxyl group (–OH) and the nitrogen atom (N) in the PNIPAM segment is also confirmed by FTIR analysis (Fig. S4, seeing in Supporting Information), since the N–H stretching vibration at 1542 cm^{-1} is greatly decreased. Concerning on the hydroxyl group (–OH) and the hydrophobic nature of 1-phenylethanol and benzyl alcohol, therefore we deem that the encapsulation of alcohol within the porous PNIPAM-*co*-PMACHE hydrogel is partly due to the hydrogen bonding and is partly ascribed to the hydrophobic–hydrophobic interaction between alcohol and the hydrogel network.

3.2. Synthesis and characterization of size-controlled Au nanoparticles within the PNIPAM-co-PMACHE hydrogel

IDA is a strong ligand which can coordinate with various transitional metal ions [39], and we have also used IDA-contained

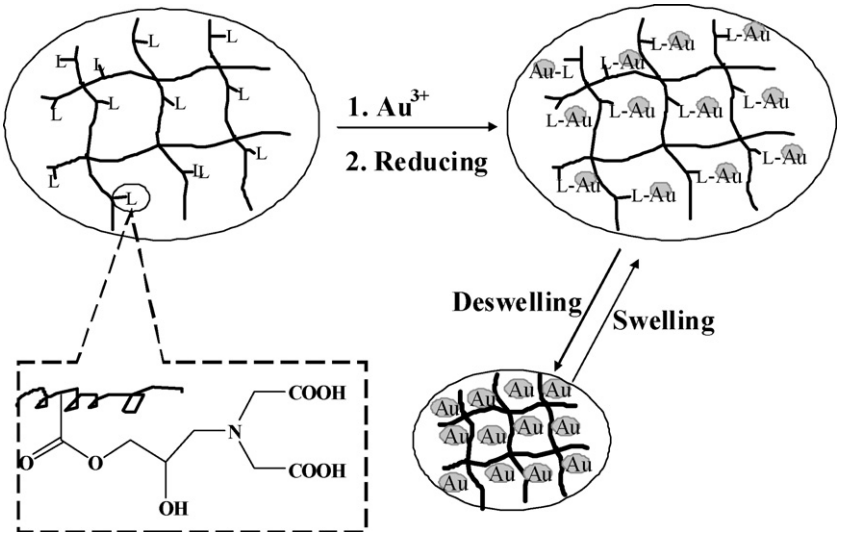

Scheme 1. Synthesis of Au nanoparticles encapsulated within the PNIPAM-*co*-PMACHE hydrogel and the reversible deswelling/swelling of the thermoresponsive hydrogel/Au composite.

polymeric materials as scaffold to immobilize Pd [40,41] and Au [31] catalyst. As discussed above, the PNIPAM-*co*-PMACHE hydrogel, which has a porous structure and contains a chelating ligand of IDA, provides the potential of nucleation and growth of metal nanoparticles within the swollen hydrogel network. Thus, Au nanoparticles are synthesized firstly by coordination of the Au precursor with the ligand of IDA and followed by reduction with a suitable reducing agent such as $NaBH_4$, sodium citrate or H_2 as shown in Scheme 1.

It is well documented that UV–vis spectroscopy can be used to diagnose the aggregation state of Au nanoparticles [42]. For example, highly dispersed 5–20 nm gold particles exhibit an absorbance peak at ~520 nm. As the gold particle size decreases, a hypsochromic shift of the characteristic absorbance occurs. When the size of gold nanoparticles further decreases to less than 3 nm, no sharp absorbance peak is observed within the UV–vis range. Fig. 3A and B shows the UV–vis absorption spectra of the hydrogel and the composite of the hydrogel and the encapsulated 2.6 nm Au nanoparticles, respectively. Compared with Fig. 3A, a distinct absorption peak around 520 nm is observed in Fig. 3B, indicating formation of Au nanoparticles [42]. From the TEM image and the inset histogram of the size distribution of the Au nanoparticles shown in Fig. 4A, it is confirmed that 2.6 nm Au nanoparticles are synthesized within the hydrogel matrix. Herein, it should be pointed out that the TEM images are obtained only for the encapsulate Au nanoparticles under the present experiment.

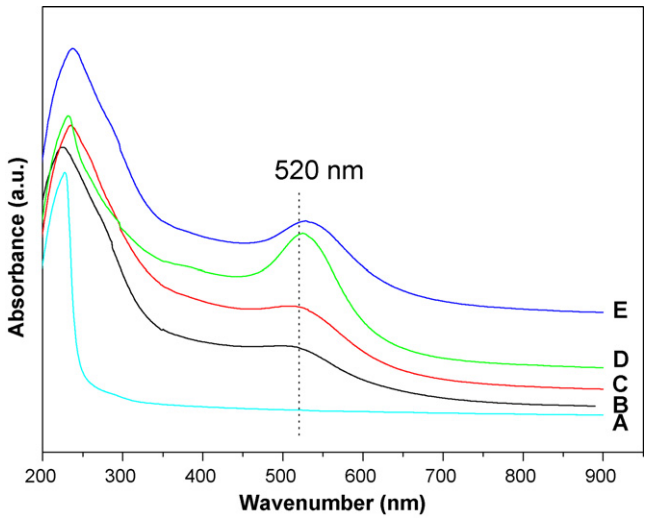

Fig. 3. The UV–vis spectra of the PNIPAM-*co*-PMACHE hydrogel (A) and the 2.6 nm (B), 4.0 nm (C), 5.7 nm (D) and 6.3 nm (E) Au nanoparticles encapsulated within the PNIPAM-*co*-PMACHE hydrogel.

It is deemed that faster nucleation favors formation of smaller nanoparticles during reduction of metal precursors [43–45]. Herein, it is found that when a diluting aqueous solution of 3.0 mmol/L $NaBH_4$ is used as reducing agent, 4.0 nm Au nanoparticles are synthesized (Fig. 4B). When the other two reducing reagents such as sodium citrate and H_2 are used to reduce the Au precursor, 5.7 and 6.3 nm Au nanoparticles are synthesized (Fig. 4), respectively. Clearly, as shown in Fig. 3 all these composites of hydrogel and the encapsulated Au nanoparticles show distinct absorption peaks ranging from 520 to 530 nm. Besides, blue shift of the characteristic absorption peaks of the composites is also observed when the size of the encapsulated Au nanoparticles increases from 2.6 to 6.3 nm.

As similar as Au nanoparticles stabilized with general PNIPAM-based hydrogel [21], the present Au nanoparticles encapsulated within the PNIPAM-*co*-PMACHE hydrogel are also thermoresponsive. As shown in Fig. 2B, the VPTT of the composite of hydrogel/Au is 27 °C, which is a little lower than those of the hydrogel itself. The little lower VPTT of the composite is possibly due to the relatively strong interaction between the encapsulated Au nanoparticles and the hydrogel, which is as similar as those reported by Ding and coworkers [46]. Besides, since the PMACHE segment is partly ionized by the basic reducing agent of $NaBH_4$ aqueous during synthesis of the Au nanoparticles, this ionization may also contribute to the lower VPTT of the composite. To explore the thermal stability of the encapsulated Au nanoparticles, the typical composite of the hydrogel and the encapsulated 6.3 nm Au nanoparticles is first heated at temperature of 80 °C and kept at that temperature for 2 h and then the composite is cooled at room temperature overnight. During this process, the deswelling/swelling of the composite is observed and the UV–vis absorption spectra of the composite are recorded. When the composite of hydrogel/Au is heated at 80 °C, part water is expelled from the composite and the newly emerging water phase lies in the upper of glass vessel, and the composite deswells and the purple deswelled composite lies in the lower layer. When temperature decreases to room temperature, water

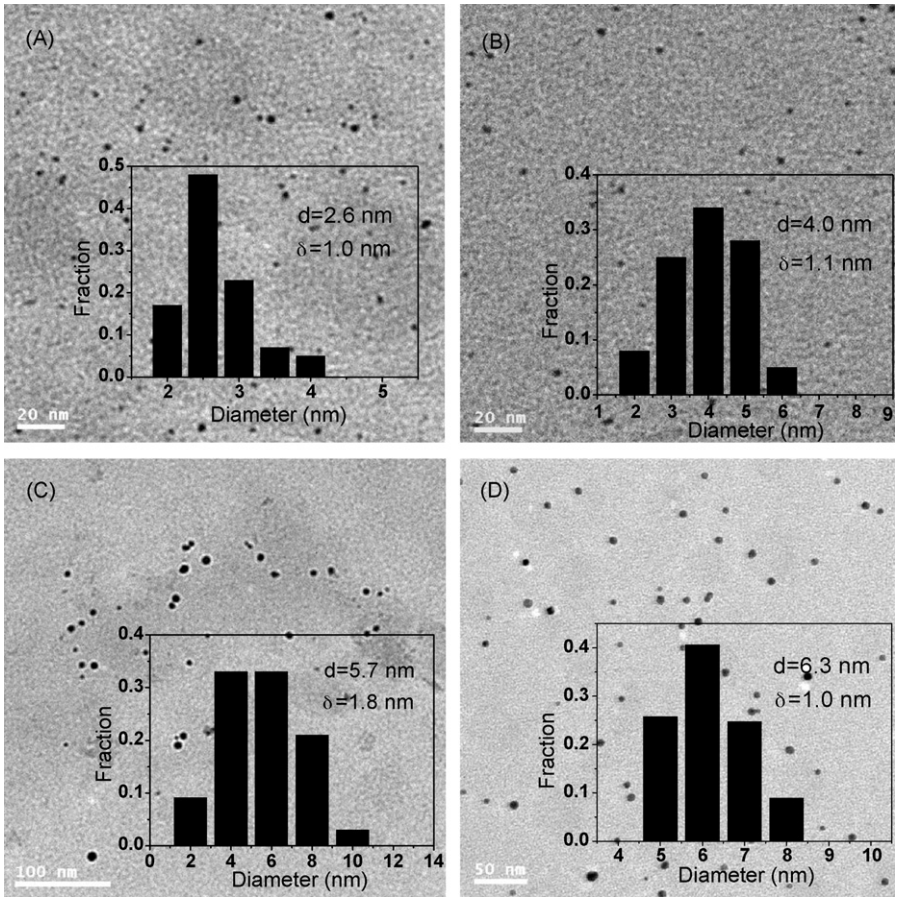

Fig. 4. TEM images of the 2.6 nm (A), 4.0 nm (B), 5.7 nm (C) and 6.3 nm (D) Au nanoparticles encapsulated within the PNIPAM-*co*-PMACHE hydrogel. Insets: the histogram of size distribution and size standard error δ of the encapsulated Au nanoparticles, in which above 200 nanoparticles are statistically calculated.

is reversibly adsorbed into the hydrogel and the deswelled composite recovers as shown in the inset in Fig. 5. It is found that the composite keeps purple after 10 heating/cooling cycles. Besides, it is also found that even when the composite is freeze-dried, it keeps purple (Fig. S6, seeing in Supporting Information). The UV–vis spectra of the composite shown in Fig. 5 indicate that the distinct absorption peak almost keeps at a constant of ~530 nm during the deswelling/swelling processes. TEM observation also indicates that the average size of the encapsulated Au nanoparticles in the recovered composite is almost as same as those in the fresh one. These results suggest that no conglomeration of Au nanoparticles occurs during the reversible deswelling/swelling of the thermoresponsive composite. We think the thermal stability of the encapsulated Au nanoparticles is mainly ascribed to the crossed-linked hydrogel network as shown in Scheme 1, which prevents conglomeration of the encapsulated Au nanoparticles. Clearly, the thermal stability of the encapsulated Au nanoparticles provides great benefit to separate and reuse of the hydrogel/Au composite.

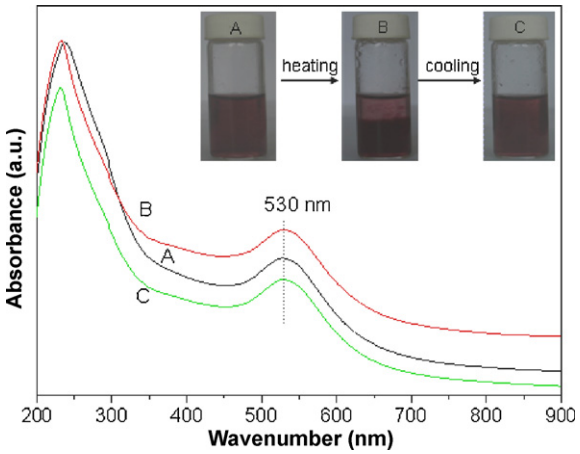

Fig. 5. The UV–vis spectra of the composite of hydrogel and encapsulated 6.3 nm Au nanoparticles. Samples: fresh sample at room temperature (A), the sample from A by heating at 80 °C (B), and the recovered sample from B by cooling at room temperature (C). Insets: optical images of the composite of the hydrogel and the encapsulated 6.3 nm Au nanoparticles.

The hydrogel/Au composite is further characterized by XPS. It is found that the gold atoms in the composite are in the metallic state since there is only one peak in the Au $4f_{7/2}$ and $4f_{5/2}$ regions. Besides, from the two typical XPS spectra of the 2.6 and 6.3 nm Au nanoparticles encapsulated within the hydrogel shown in Fig. 6, the Au 4f binding energies ($4f_{7/2}$, 82.9–83.4 eV and $4f_{5/2}$, 86.6–86.8 eV) are lower than those of the general supported Au nanoparticles [47], indicating that there exists strong interaction between the Au nanoparticles and the hydrogel [48,49]. Clearly, the strong interaction between the Au nanoparticles and the hydrogel is also verified by the lower VPTT of the hydrogel/Au composite as discussed above.

3.3. Aerobic alcohol oxidation catalyzed by the encapsulated Au nanoparticles

Size-sensitive and size-dependent catalysis of noble metal nanoparticles stimulates extensive attention since it is useful to explore the catalytic mechanism [2,7,19,50]. As to Au nanocatalyst, its size-selective catalysis in CO oxidation [51] and hydrogena-

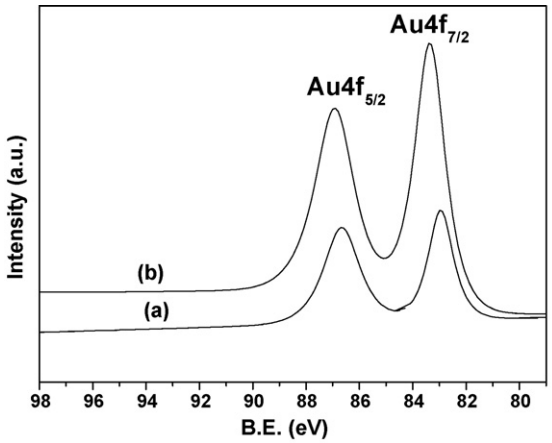

Fig. 6. The Au 4f XPS spectra of the 2.6 nm (a) and 6.3 nm (b) Au nanoparticles encapsulated within the PNIPAM-*co*-PMACHE hydrogel.

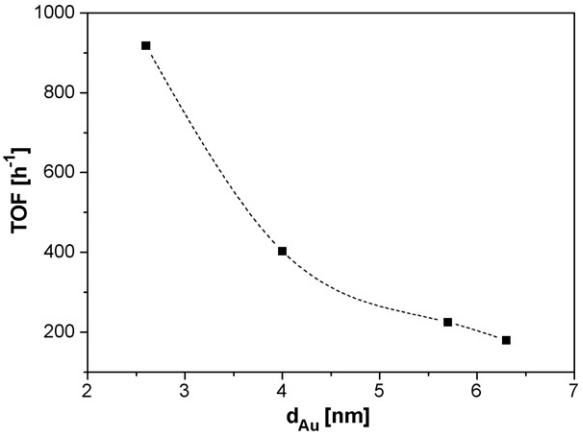

Fig. 8. The size dependence of the TOF value of the encapsulated Au nanoparticles for the aerobic oxidation of 1-phenylethanol. See reaction conditions in Fig. 7.

tion [52–54] has been reported. For aerobic oxidation of alcohol with molecular oxygen by Au nanocatalyst, it is thought that the activity and selectivity of Au nanocatalyst is determined by various factors such as the size of Au nanoparticles [2,7,19,50], the interaction between Au nanoparticles and the support material [55], the nature of the support material [56], and the preparation method of Au nanocatalyst [7], although a detailed mechanism of alcohol oxidation on Au nanoparticles has not been concluded [57]. Of all these factors, it is generally deemed that the size of Au nanoparticles is important for aerobic alcohol oxidation. Herein, the catalytic activity of the hydrogel/Au composite with different size of encapsulated Au nanoparticles is tested. Besides, to eliminate the effect of Au nanocatalyst content on catalytic efficiency, the same weight of the hydrogel/Au composite containing the same amount of Au nanocatalyst (15 g of the composite containing 6.0×10^{-4} mmol of Au nanocatalyst) is employed in all the oxidations performed at 80 °C.

Fig. 7A shows the time dependence yield of acetophenone for aerobic oxidation of 1-phenylethanol at 80 °C catalyzed by the encapsulated 2.6 nm Au nanoparticles. The yield quickly increases to 65% in 1 h and further gradually increases until a quantitative yield is achieved in 6 h. The 2.6 nm Au nanocatalyst affords a turnover frequency (TOF) value of 9.2×10^2 h^{-1}, which is calculated by total Au atoms. As similar as the 2.6 nm Au nanocatalyst, the TOF values of the other three catalysts of 4.0, 5.7 and 6.3 nm Au nanoparticles for aerobic oxidation of 1-phenylethanol are also calculated based on the inset in Fig. 7, and the results are shown in Fig. 8.

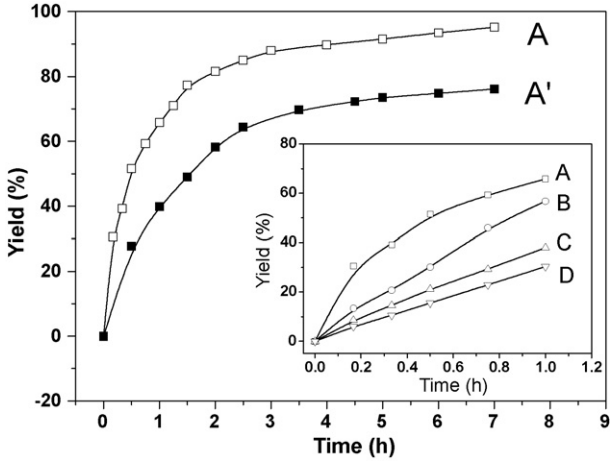

Fig. 7. The time-yield plots for 1-phenylethanol oxidation employing 0.20 mol% of the encapsulated 2.6 nm Au nanocatalyst at 80 °C (A), and 1.0 mol% of the 2.6 nm Au nanocatalyst at 27 °C (A′). Insets: the initial time-yielding plots for 1-phenylethanol oxidation employing 0.20 mol% of the 2.6 nm (A), 4.0 nm (B), 5.7 nm (C) and 6.3 nm (D) Au nanocatalysts at 80 °C. Reaction conditions: 3.0 mmol of 1-phenylethanol, 9.0 mmol of KOH, 15 g of swollen hydrogel/Au composite containing 0.20 or 1.0 mol% Au nanocatalyst, O_2 at bubbling 0.05 L/min, HPLC yield.

As shown in Fig. 8, the TOF value depends significantly on the average size of the encapsulated Au nanoparticles. That is to say, in the size range from 2.6 to 6.3 nm the smaller size of Au nanoparticles, the higher TOF value and therefore the faster alcohol oxidation. For example, TOF value decreases from 9.2×10^2 to 1.8×10^2 h^{-1} when the average size of the encapsulated Au nanoparticles increases from 2.6 to 6.3 nm. These results confirm size-dependent catalysis of the present Au nanocatalyst for aerobic oxidation of 1-phenylethanol. Herein, it should be pointed out that Au nanoparticles with size smaller than 2.6 nm are not synthesized, partly since it has been reported that Au nanoparticles smaller than 3 nm are apt to agglomerate during oxidation and therefore eventually influences the catalytic performance of the Au nanocatalyst [58].

Recently, several elegant Au nanocatalysts are proposed for aerobic alcohol oxidation on mild conditions such as at room temperature [2,4]. Herein, the aerobic oxidation of 1-phenylethanol catalyzed by 1.0 mol% of the encapsulated 2.6 nm Au nanoparticles at 27 °C is studied. As shown in Fig. 7A′, the aerobic oxidation of 1-phenylethanol runs smoothly at 27 °C and affords a relatively high TOF value of 55 h^{-1}, and 60% yield is achieved in 2 h.

Bergbreiter et al. has proposed a PNIPAM-based thermomorphic system for organic synthesis [59]. This thermomorphic system employs the phase-selective solubility of PNIPAM in binary or ternary organic solvent mixture to facilitate catalyst recycling and product separation. Besides, some other PNIPAM-based thermoresponsive polymeric materials such as microgel [29–31] are also used to immobilize noble metal catalyst. Compared with the general PNIPAM-based thermomorphic system, besides the advantage of easy catalyst recycling which will be discussed subsequently, the present hydrogel/Au composite has other advantages. First, synthesis of the present PNIPAM-*co*-PMACHE hydrogel is easy. As discussed in the experimental section, the polymerization is performed on very mild condition, and the two monomers are almost quantitatively converted, and high yield of bulk hydrogel is achieved. Second, no organic cosolvent is needed in the present catalysis since the porous hydrogel network has the ability to encapsulate the hydrophobic reactant of alcohol. Herein, it should be pointed out that no other solvent but the hydrogel/Au com-

posite is added during the aerobic alcohol oxidation. The hydrogel acts as not only scaffold of the Au nanocatalyst but also the reaction medium. Since the present composite is composed of ~99 wt% water, therefore it can be deemed that the alcohol oxidation is performed in water. Third, the alcohol oxidation can be accelerated through the reversible deswelling/deswelling of the composite. As discussed above, when alcohol is mixed with the hydrogel/Au composite, the alcohol is encapsulated within the hydrogel network. The encapsulated alcohol is further concentrated within the hydrogel network when the base of KOH is added or the mixture is heated above VPTT of the composite. In fact, at the reaction temperature of 80 °C, the composite deswells and most of water is squeezed out, and therefore the encapsulated alcohol is concentrated. It is found that the composite containing the encapsulated alcohol deswells from 15.4 g (15 g of composite and 0.36 g of 1-phenylethanol) to 1 g (approximately estimated by gravimetrical measurement), indicating that the encapsulated 1-phenylethanol and the Au nanocatalyst is 15 times concentrated. As is known that the Au-catalyzed alcohol oxidation follows the Langmuir–Hinselwood reaction mechanism, that is, the higher concentration of the reactants in a confined range, the faster the reaction, therefore we expect that the present alcohol oxidation can be accelerated by the deswelling of the thermoresponsive composite. Fourth, there exists strong hydrogen bonding between the alcohol molecules and the PNIPAM segment, therefore the hydroxy group (–OH) of the alcohol is possibly activated and alcohol oxidation is promoted. Besides, we also suppose that the strong interaction between the Au nanoparticles and the hydrogel, which is confirmed by the low Au 4f binding energies and low VPTT of the hydrogel/Au composite as discussed above, also contribute high catalytic activity of the Au nanocatalyst, although the reason needs further exploration.

Lastly, recycling of the composite of the hydrogel and the encapsulated 2.6 nm Au nanoparticles is discussed. As similar as the hydrogel/Pd composite introduced in the previous manuscript [33], the present hydrogel/Au composite can reversibly deswell/swell to give response to temperature change. It is found that the separation of the present composite from the reaction mixture is such an easy thing. After the synthesized product is extracted with diethyl ether, the composite is firstly heated above VPTT and the composite deswells, then the deswelled composite can be separated by simple filtration at that temperature. The deswelled composite can be easily recovered by swelling in water at room temperature. However, since no by-product other than H_2O is produced and no reactant other than O_2 is consumed during the aerobic oxidation, it is not necessary to separate the composite in the present study. Therefore, after the extraction of the synthesized product with diethyl ether, the composite is directly reused in the next run of oxidation without additional treatment. As shown in Fig. 9, after 4 times of catalyst recycling, the yield of acetophenone almost keeps a constant, suggesting that the recovered composite is almost as catalytically efficient as the fresh one. To explore possible leaching of the Au nanocatalyst into the ether phase during the extraction, analysis of the organic phase is also made by AAS and leaching Au catalyst is not detected.

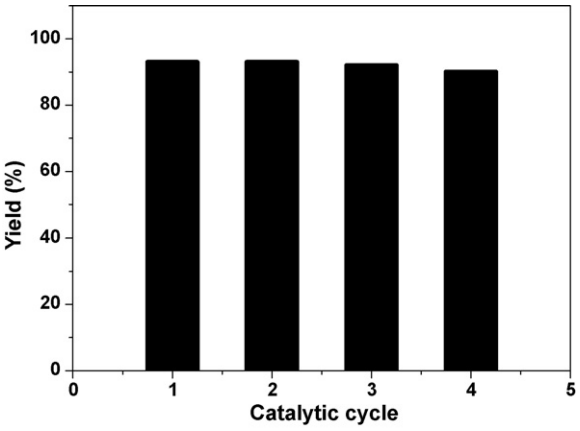

Fig. 9. Recycling of the hydrogel/Au composite for aerobic oxidation of 1-phenylethanol. Reaction conditions: 3.0 mmol of 1-phenylethanol, 9.0 mmol of KOH, 15 g of swollen hydrogel/Au composite containing 0.20 mol% of 2.6 nm Au nanoparticles, bubbling O_2 at 0.05 L/min, 80 °C, 6 h, HPLC yield.

4. Conclusions

Synthesis of size-controlled Au nanoparticles for aerobic alcohol oxidation within a porous, chelating and intelligent hydrogel of PNIPAM-*co*-PMACHE, which contains a thermoresponsive segment of PNIPAM and a chelating segment of PMACHE, is studied. The PNIPAM-*co*-PMACHE hydrogel is demonstrated to be a suitable scaffold, within which Au nanoparticles with size ranging from 2.6 to 6.3 nm are synthesized by reducing the Au precursor with different reducing agents. The synthesized composite of the hydrogel and the encapsulated Au nanoparticles can reversibly deswell/swell at the volume-phase-transition temperature (VPTT) as similar as the hydrogel itself. The encapsulated Au nanoparticles keep stable and no conglomeration occurs during the reversible deswelling/swelling of the hydrogel/Au composite, which therefore provides great convenience for catalyst recycling. The catalytic activity of the encapsulated Au nanoparticles for aerobic alcohol oxidation is studied. It is found that the catalyst activity is strongly dependent on the size of the encapsulated Au nanoparticles. That is, the TOF value decreases with the increase in the size of the encapsulated Au nanoparticles in the range from 2.6 to 6.3 nm. It is demonstrated that the catalyst of 2.6 nm Au nanoparticles encapsulated within the PNIPAM-*co*-PMACHE hydrogel is highly efficient and reusable catalyst for aerobic alcohol oxidation. Besides, the reason ascribed to the high catalytic efficiency of the encapsulated Au nanoparticles is discussed.

Acknowledgements

The financial support by National Science Foundation of China (No. 20974051), Tianjin Natural Science Foundation (No. 09JCYBJC02800), and the Program for New Century Excellent Talents in University (No. NCET-06-0216) is gratefully acknowledged.

Appendix A. Supplementary data

Supplementary data associated with this article can be found, in the online version, at doi:10.1016/j.molcata.2009.10.026.

References

[1] D.G. Lee, U.A. Spitzer, J. Org. Chem. 35 (1970) 3589.
[2] H. Tsunoyama, H. Sakurai, Y. Negishi, T. Tsukuda, J. Am. Chem. Soc. 127 (2005) 9374.
[3] Y.M.A. Yamada, T. Arakawa, H. Hocke, Y. Uozumi, Angew. Chem. Int. Ed. 46 (2007) 704.
[4] S. Kanaoka, N. Yagi, Y. Fukuyama, S. Aoshima, H. Tsunoyama, T. Tsukuda, H. Sakurai, J. Am. Chem. Soc. 129 (2007) 12060.
[5] H. Miyamura, R. Matsubara, Y. Miyazaki, S. Kobayashi, Angew. Chem. Int. Ed. 46 (2007) 4151.
[6] F. Porta, L. Prati, J. Catal. 224 (2004) 397.
[7] (a) A. Abad, P. Concepcion, A. Corma, H. Garcia, Angew. Chem. Int. Ed. 44 (2005) 4066;
(b) A. Abad, A. Corma, H. Garcia, Chem. Eur. J. 14 (2008) 212.
[8] P. Haider, J.-D. Grunwaldt, R. Seidel, A. Baiker, J. Catal. 250 (2007) 313.
[9] D. Ferri, C. Mondelli, F. Krumeich, A. Baiker, J. Phys. Chem. B 110 (2006) 22982.
[10] J. Chen, Q. Zhang, Y. Wang, H. Wan, Adv. Synth. Catal. 350 (2008) 453.
[11] K. Ebitani, Y. Fujie, K. Kaneda, Langmuir 15 (1999) 3557.
[12] T. Mallat, A. Baiker, Catal. Today 19 (1994) 247.
[13] A. Biffis, L. Minati, J. Catal. 236 (2005) 405.

[14] Z. Opre, J.-D. Grunwaldt, M. Maciejewski, D. Ferri, T. Mallat, A. Baiker, J. Catal. 230 (2005) 406.
[15] K. Yamaguchi, N. Mizuno, Angew. Chem. Int. Ed. 41 (2002) 4538.
[16] X. Yang, X. Wang, C. Liang, W. Su, C. Wang, Z. Feng, C. Li, J. Qiu, Catal. Commun. 9 (2008) 2278.
[17] L.-C. Wang, L. He, Q. Liu, Y.-M. Liu, M. Chen, Y. Cao, H.-Y. He, K.-N. Fan, Appl. Catal. A: Gen. 344 (2008) 150.
[18] C. Burato, P. Centomo, G. Pace, M. Favaro, L. Prati, B. Corain, J. Mol. Catal. A: Chem. 238 (2005) 26.
[19] H. Tsunoyama, H. Sakurai, T. Tsukuda, Chem. Phys. Lett. 429 (2006) 528.
[20] L. Delannoy, N. Weiher, N. Tsapatsaris, A.M. Beesley, L. Nchari, S.L.M. Schroeder, C. Louis, Top. Catal. 44 (2007) 263.
[21] (a) H. Tokuyama, A. Kanehara, React. Funct. Polym. 67 (2007) 136;
(b) Z. Wang, B. Tan, I. Hussain, N. Schaeffer, M.F. Wyatt, M. Brust, A.I. Cooper, Langmuir 23 (2007) 885;
(c) J.-H. Kim, T.R. Lee, Langmuir 23 (2007) 6504;
(d) C. Wang, N.T. Flynn, R. Langer, Adv. Mater. 16 (2004) 1074;
(e) F.Y. Pong, M. Lee, J.R. Bell, N.T. Flynn, Langmuir 22 (2006) 3851.
[22] (a) Y.M. Mohan, T. Premkumar, K. Lee, K.E. Geckeler, Macromol. Rapid Commun. 27 (2006) 1346;
(b) P. Saravanan, M.P. Raju, S. Alam, Mater. Chem. Phys. 103 (2007) 278;
(c) Y. Lu, P. Spyra, Y. Mei, M. Ballauff, A. Pich, Macromol. Chem. Phys. 208 (2007) 254.
[23] (a) K.S. Sivudu, N.M. Reddy, M.N. Prasad, K.M. Raju, Y.M. Mohan, J.S. Yadav, G. Sabitha, D. Shailaja, J. Mol. Catal. A: Chem. 295 (2008) 10;
(b) S.E. Kudaibergenov, Z.E. Ibraeva, N.A. Dolya, B.K. Musabaeva, A.K. Zharmagambetova, J. Koetz, Macromol. Symp. 274 (2008) 11.
[24] (a) D. Palioura, S.P. Armes, S.H. Anastasiadis, M. Vamvakaki, Langmuir 23 (2007) 5761;
(b) N.M. El-Ashgar, I.M. El-Nahhal, M.M. Chehimi, F. Babonneau, J. Livage, Mater. Lett. 61 (2007) 4553.
[25] G. Iyer, P. Iyer, L.M.V. Tillekeratne, M.R. Coleman, A. Nadarajah, Macromolecules 40 (2007) 5850.
[26] S. Kim, K.E. Healy, Biomacromolecules 4 (2003) 1214.
[27] M. Ebara, T. Aoyagi, K. Sakai, T. Okano, Macromolecules 33 (2000) 8312.
[28] E. Diez-Pena, I. Quijada-Garrido, J.M. Barrales-Rienda, Macromolecules 35 (2002) 8882.
[29] Y. Lu, S. Proch, M. Schrinner, M. Drechsler, R. Kempe, M. Ballauff, J. Mater. Chem. 19 (2009) 3955.
[30] A. Biffs, N. Orlandi, B. Corain, Adv. Mater. 15 (2003) 1551.
[31] X. Jiang, D. Xiong, Y. An, P. Zheng, W. Zhang, L. Shi, J. Polym. Sci. Part A: Polym. Chem. 45 (2007) 2812.
[32] (a) R. Valentin, K. Molvinger, C. Viton, A. Domard, F. Quignard, Biomacromolecules 6 (2005) 2785;
(b) B. Corain, K. Jerabek, P. Centomo, P. Canton, Angew. Chem. Int. Ed. 43 (2004) 959.
[33] Y. Wang, J. Zhang, W. Zhang, M. Zhang, J. Org. Chem. 74 (2009) 1923.
[34] (a) W. Hyk, M. Ciszkowska, J. Phys. Chem. B 106 (2002) 11469;
(b) K. Lszl, K. Kosik, C. Rochas, E. Geissler, Macromolecules 36 (2003) 7771.
[35] G. Wei, W. Zhang, F. Wen, Y. Wang, M. Zhang, J. Phys. Chem. C 112 (2008) 10827.
[36] T. Kawashima, S. Koga, M. Annaka, S. Sasaki, J. Phys. Chem. B 109 (2005) 1055.
[37] C.S. Brazel, N.A. Peppas, Macromolecules 28 (1995) 8016.
[38] M. Shibayama, S. Mizutani, B. Nomura, Macromolecules 29 (1996) 2019.
[39] F.G. Vilchez, M. Castillo-Martos, M.F. Gargallo, Transit. Met. Chem. 2 (1977) 67.
[40] J. Zhang, W. Zhang, Y. Wang, M. Zhang, Adv. Synth. Catal. 350 (2008) 2065.
[41] M. Zhang, W. Zhang, J. Phys. Chem. C 112 (2008) 6245.
[42] (a) P.B. Johnson, R.W. Christy, Phys. Chem. B 6 (1972) 4370;
(b) T.R. Jensen, M.L. Duval, K.L. Kelly, A.A. Lazarides, G.C. Schatz, R.P.V. Duyne, J. Phys. Chem. B 103 (1999) 9846.
[43] (a) J. Turkevich, P.C. Stevenson, J. Hillier, Discuss. Faraday Soc. 11 (1951) 55;
(b) B.V. Enustun, J. Turkevich, J. Am. Chem. Soc. 85 (1963) 3317.
[44] (a) R. Zanella, S. Giorgio, C.R. Henry, C. Louis, J. Phys. Chem. B 106 (2002) 7634;
(b) R. Zanella, S. Giorgio, C.H. Shin, C.R. Henry, C. Louis, J. Catal. 222 (2004) 357.
[45] R.M. Rioux, H. Song, J.D. Hoefelmeyer, P. Yang, G.A. Somorjai, J. Phys. Chem. B 109 (2005) 2192.
[46] X. Zhao, X. Ding, Z. Deng, Z. Zheng, Y. Peng, C. Tian, X. Long, New J. Chem. 30 (2006) 915.
[47] T. Herranz, X. Deng, A. Cabot, P. Alivisatos, Z. Liu, G. Soler-Illia, M. Salmeron, Catal. Today 143 (2009) 158.
[48] H. Tsunoyama, N. Ichikuni, H. Sakurai, T. Tsukuda, J. Am. Chem. Soc. 131 (2009) 7086.
[49] P. Tripathy, A. Mishra, S. Ram, H.-J. Fecht, J. Bansmann, R.J. Behm, Nanotechnology 20 (2009) 075701.
[50] M. Comotti, C.D. Pina, R. Matarrese, M. Rossi, Angew. Chem. Int. Ed. 43 (2004) 5812.
[51] S.H. Overbury, V. Schwartz, D.R. Mullins, W. Yan, S. Dai, J. Catal. 241 (2006) 56.
[52] J. Jia, K. Haraki, J.N. Kondo, K. Domen, K. Tamaru, J. Phys. Chem. B 104 (2000) 11153.
[53] C. Milone, R. Ingoglia, A. Pistone, G. Neri, F. Frusteri, S. Galvagno, J. Catal. 222 (2004) 348.
[54] S. Panigrahi, S. Basu, S. Praharaj, S. Pande, S. Jana, A. Pal, S.K. Ghosh, T. Pal, J. Phys. Chem. C 111 (2007) 4596.
[55] D.I. Enache, D.W. Knight, G.J. Hutchings, Catal. Lett. 103 (2005) 43.
[56] L.-C. Wang, Y.-M. Liu, M. Chen, Y. Cao, H.-Y. He, K.-N. Fan, J. Phys. Chem. C 112 (2008) 6981.
[57] (a) T. Mallat, A. Baiker, Chem. Rev. 104 (2004) 3037;
(b) T. Matsumoto, M. Ueno, N. Wang, S. Kobayashi, Chem. Asian J. 3 (2008) 196.
[58] (a) M. Haruta, M. Daté, Appl. Catal. A: Gen. 222 (2001) 427;
(b) M. Valden, X. Lai, D.W. Goodman, Science 281 (1998) 1647.
[59] (a) D.E. Bergbreiter, S.D. Sung, Adv. Synth. Catal. 348 (2006) 1352;
(b) D.E. Bergbreiter, P.L. Osburn, J.D. Frels, J. Am. Chem. Soc. 123 (2001) 11105;
(c) D.E. Bergbreiter, P.L. Osburn, T. Smith, C. Li, J.D. Frels, J. Am. Chem. Soc. 125 (2003) 6254.